Nat. Hazards Earth Syst. Sci. Discuss., 3, C1901–C1913, 2015
www.nat-hazards-earth-syst-sci-discuss.net/3/C1901/2015/
© Author(s) 2015. This work is distributed under
the Creative Commons Attribute 3.0 License.

Natural Hazards and Earth System Sciences
Discussions

Interactive comment on "Probabilistic tsunami hazard assessment for the Makran region with focus on maximum magnitude assumption" *by* A. Hoechner et al.

A. Hoechner et al.

hoechner@gfz-potsdam.de

Received and published: 6 October 2015

Following points were identified in the comments by anonymous referee #1:

1. Figure of slab profile and comment on assumptions
2. Seismicity analysis
3. Earthquake interaction in space and time
4. Synthetic catalog stability
5. Elaborate on hypocenter/barycenter, scaling relations and slip distribution

6. Application of Green's law
7. Computation of percentiles and probabilistic tsunami height PTH
8. Comparison to previous study
9. Huge dependence of POE on max. magnitude problematic for decision makers

We will now respond to the questions and requests and will modify the final paper accordingly either in the maint text or as supplementary material.

1. Figure of slab profile and comment on assumptions

As mentioned in the paper, the Makran geometry is neither available via the RUM model (Gudmundsson and Sambridge, 1998) nor Slab1.0 (Hayes et al., 2012). The best we could come up with is a profile from Smith et al. (2013, figure 2a), which is based on a combination of seismic reflection lines, and which the authors employed for their thermo-mechanical modeling. The profile is shown in map and side view in Fig. 1 (solid red line). We slightly shifted the profile (dashed line) and rotated it so as to match the deformation front (blue line) from the same publication (figure 1 therein). This results in the 3d geometry as shown in Fig. 1 in green (rectangles are the earthquake- and tsunami subfaults for the Green's functions).

Of course, this approach is by no means providing an accurate, final model of the subduction interface. Many more data and studies are highly desirable to get a better understanding of the structure (as well as the activity) at the Makran. Hazard models based on other geometry assumptions could be made, but taking into account geometric complications or variations is outside the scope of the present study, where the focus is on the effect of seismicity, and especially maximum magnitude assumptions.

2. Seismicity analysis

We agree that the time span of the seismic data in this case is too short to get robust estimates of the seismic activity for the Makran (and even more so if further spatial

subdivision is aspired to), especially concerning maximum magnitude. This is why we try to specifically address this problem in the present study.

3. Earthquake interaction in space and time

The temporal and spatial interplay of earthquakes is a complicated process which has to be considered, for instance, if simulations of the earthquake cycle are carried out. In this study however, we can assume that for a long time span, the average slip will be similar across the interface (homogeneous plate coupling assumed). Temporal clustering is actually irrelevant for our hazard computations, since only the total time span of the catalog is used therefore.

4. Synthetic catalog stability

The reviewer raises the possibility that there might be too few large events in the synthetic catalog to get stable hazard estimates based on figure 2 (left panel) in the paper. In that figure, the event hypocenters are plotted in chronological order, so that the rare large events are covered by the more frequent small events. Here, in Fig. 2 we plot the same catalog (also 75 ky) but sort the events by size (largest on top). Additionally, in the right panel we plot the whole 300 ky, but only above magnitude Mw=8. This shows that indeed there should be sufficient events to guarantee stable results, especially considering that these larger events have significant spatial extension leading to quite homogeneous coverage.

To make sure, we generated additional test catalogs with the same parameterization as the reference catalog and computed the hazard. These technical results, which were not presented in the paper, but will be added as a supplement, are shown here in Fig. 3. The variation is small and agrees well with the expected distribution from the percentiles.

5. Elaborate on hypocenter/barycenter, scaling relations and slip distribution

There are several suggestions in the literature concerning scaling relations for earth-

quake extension. The most frequently used relationship is probably the one by Wells and Coppersmith (1994). We select the proposition by Blaser et al. (2010) (reverse orthogonal), which is based on a more recent data set and tailored to larger subduction events. A subfault is activated if the distance of its center to the hypocenter falls within the empirical scaling relation. Along dip, the strength of the activation is determined by the formula by Geist and Dmowska (1999) (symmetrical), which is analytically derived based on some physical assumptions and leads to a bell-shaped slip distribution. Within 20% of the lateral edges we linearly taper the slip to zero. This means that in general, the randomly selected hypocenter is (almost) the barycenter of the slip distribution. If however the hypocenter falls close to an edge of the plate geometry, the missing moment due to fewer activated subfaults is compensated by higher slip on the other subfaults, and the slip is not tapered to zero at the edge. This can partly mimic the effect of splay-faults at the surface. In this case, the earthquake has a bit different scaling relations and the hypocenter does not correspond to the barycenter. Some examples for this deterministic procedure are shown in Fig. 4 for events of varying size.

In order to assess the effect of the scaling relations and slip distribution, we generated two additional catalogs, one where length and width were varied randomly for each event (Fig. 5), and another catalog where the slip distribution was perturbed with noise (Fig. 6). These catalogs resulted in similar tsunami hazard. The probabilistic tsunami heights for 500 and 5000 y for the reference catalog and the two variants are 9.1; 21.3 / 9.0; 22.9 / 9.3; 22.4 m.

6. Application of Green's law

Using Green's law for the estimation of tsunami coastal impact has become common practice when computing wave propagation for a very large number of scenarios. The reasoning is as follows. The number of grid elements is not able to resolve the shoaling of the wave when it approaches the coast and the wave height at the coast will be underestimated. The use of nested grids or non-regular finite-element meshes dramatically increases the computational cost. Instead, Kamigaichi (2009) demonstrated

that Green's law projection from offshore positions gives coastal wave heights similar to those computed on a much finer grid. This approach is also implemented, for example, in the Japanese Tsunami Early Warning forecasting. We extrapolate to 1 m water depth.

7. Computation of percentiles and probabilistic tsunami height PTH

First, for every point of interest along the coast (or collection of points) the number of exceedances for varying wave height levels is counted. The percentiles are calculated using the inverse cumulative Poisson distribution. For instance, if there are 150 exceedances at some point for some wave height, the 15th and 85th percentiles are 137 and 163 (Matlab: poissinv([0.15 0.85],150)). This means that 70% of random realizations of the synthetic catalog with identical parameterization will fall within these numbers.

Dividing the number of exceedances by catalog time span yields the annual rate R. The probability of exceedance for N years is again computed using Poisson statistics: P(N)=1-exp(-R*N).

We now have for every point the annual prob. of exc. as a function of wave height. The probabilistic tsunami height for some time T is computed by interpolation of the inverse relation at Pann=1/T. This results in the wave height which is on average exceeded once every T years and occurs with a probability of 1-exp(-1)$\approx$0.63 in T years one or more times.

In the paper in section 2.4 we mistakenly refer to annual probability where annual rate would be correct. As stated above, annual probability is derived using Pann=1-exp(-R).

8. Comparison to previous study

Heidarzadeh and Kijko (2010) refer to their publication as a 'first-generation study', since it contains only three earthquake scenarios of identical magnitude. This is the reason why in Table 4 therein, on the right side containing the probabilities of ex-

ceedance for 50 years, in the 36 entries there appear only four different values (whereof 20 times 0.00%). In our discussion, we selected their results which are best comparable to our study. The fact that they are compatible if interpreted as we explain (though not identical), is a confirmation for both approaches. However, our study, containing about 20'000 earthquakes per catalog, enables a finer (and hopefully more realistic) spatial and temporal assessment of the hazard. Furthermore, the different catalogs assess the effect of various factors (as maximum magnitude), which is the primary focus of our study.

9. Huge dependence of probability of exceedance on max. magnitude problematic for decision makers

The reviewer states that if all the considered maximum magnitudes were equiprobable, the resulting uncertainties in probability of exceedance POE were lethal for decision makers. For instance, according to the lower left panel in Fig. 5, for Pakistan and Iran the POE of 8 m in 500 years varies from 0% to 80% and for 15 m in 5000 years from 0% to 100%.

First of all, the maximum magnitudes shown in Fig. 5 are absolutely not equiprobable over the full range. Since we know that an event with magnitude Mw=8.1 has already happened, maximum magnitudes below that don't need to be considered. The results are shown nevertheless in order to get a better understanding of the general dependence. The maximum magnitudes on the far right side of the graphs are very improbable, since the largest earthquakes can only be fit into the subduction geometry under extreme and unrealistic assumptions, and for a failing of the whole zone at once. In the realistic range, the variation of the POE for 8 m in 500 years for Pakistan and Iran is maybe 50-70% and for 15 m in 5000 years 50-90%.

The still quite high variation of the latter reflects the steep transition necessarily occurring in a probability from something which is not possible at all (for small magnitudes) to something that is probable (and is also happening almost certainly in the long run).

A measure which is more 'linearly' dependent (that is, does not saturate) on maximum magnitude assumption than POE is the probabilistic tsunami height PTH shown in the upper panels of Fig. 5 in the paper. In the realistic range, PTH is about 7-9 m for 500 years and around 15-21 m for 5000 years, which should be manageable for decision makers.

Interactive comment on Nat. Hazards Earth Syst. Sci. Discuss., 3, 5191, 2015.

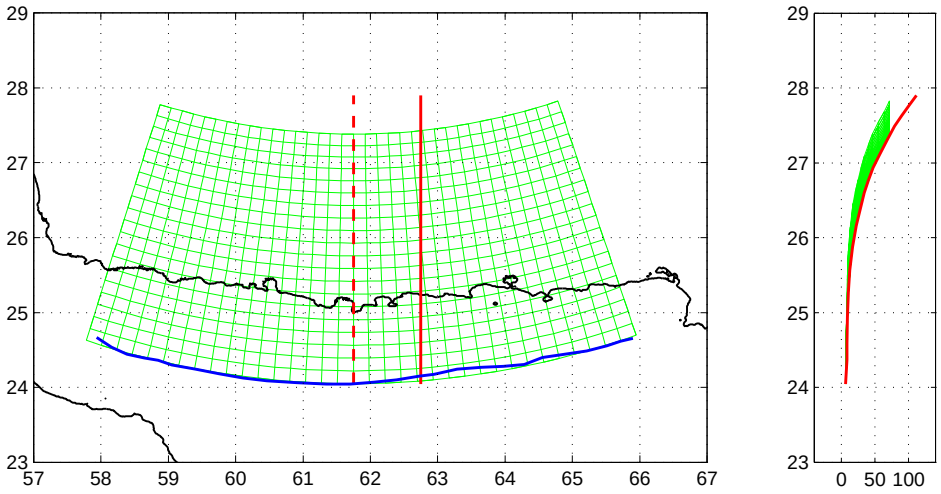

Fig. 1. Profile (red) and deformation front (blue) as from Smith et al. (2013) and constructed 3d geometry (green) as used in the present study.

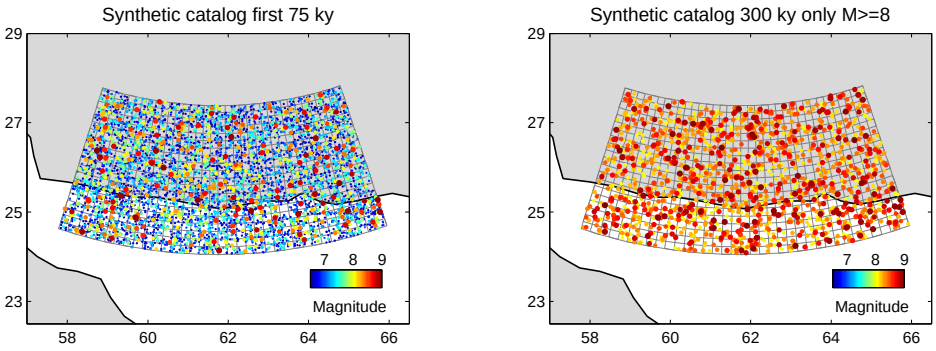

Fig. 2. Left: same plot as in paper, but synthetic catalog event hypocenters sorted by size (large on top) instead chronological. Right: Whole 300 ky of catalog above magnitude Mw=8.

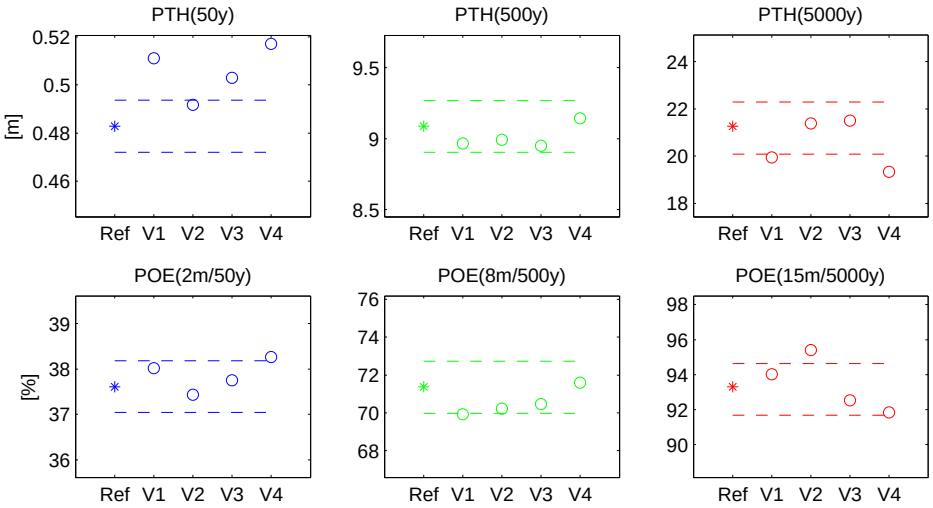

Fig. 3. Hazard results (Iran & Pakistan) for the reference synthetic catalog and four additional test catalogs (circles). Dashed: 15th and 85th percentiles.

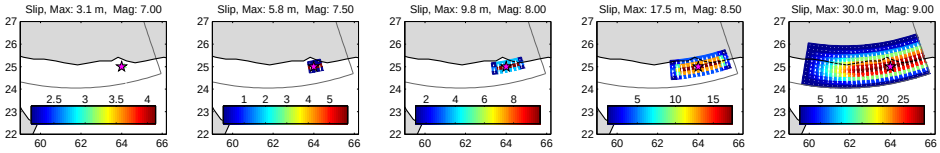

Fig. 4. Illustration of the empirical scaling relations and slip distribution used for varying earthquake size.

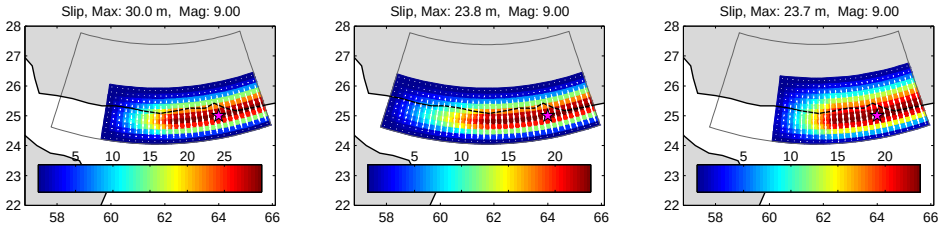

Fig. 5. Variation of the empirical scaling relations, where each event is altered randomly, but keeping the variation of length, width, their product and quotient within 30%. Left panel: reference.

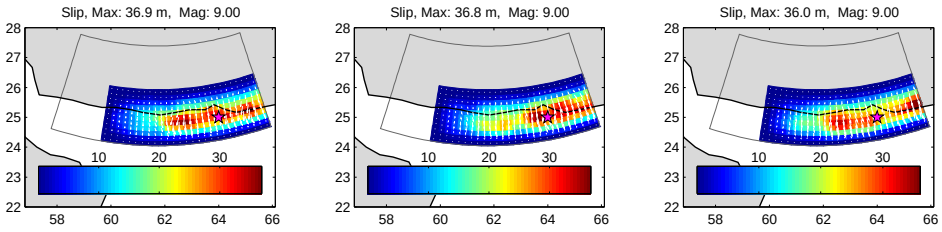

Fig. 6. Perturbation of the slip distribution (and rake angle) by multiplication with noise. The noise is generated by applying a spatial low-pass filter to a uniform random distribution.